

Dielectric properties of yeast cells as simulated by the two-shell model

Valerică Raicu^{*}, Georgeta Raicu¹, Grigore Turcu¹

Romanian Academy, Institute of Physical Chemistry, Department of Colloids, Spl., Independentei 202, 79611 Bucharest, Romania

Received 6 February 1996; accepted 18 March 1996

Abstract

The paper reports a re-evaluation of the previous studies on yeast by considering the influence of vacuole upon the dielectric properties of the whole cell. In this respect, relative permittivity and conductivity of yeast cells dispersed in KCl solutions of various concentrations were measured in the frequency range from 0.1 to 100 MHz. The analysis of data revealed that the β -dielectric dispersion of yeast cell suspensions is a composite of three (or probably four) distinct sub-dispersions. Since the dielectric response of the cell wall was experimentally avoided (according to Asami et al. (1976) *J. Membr. Biol.* 28, 169–180), the two-shell model, related to the plasma membrane and the vacuolar membrane, respectively, appeared to be the best approximation for yeast cells. The most relevant parameters obtained with the aid of the two-shell model were as follows. Specific capacitance of the plasma membrane and the vacuolar membrane were $0.703 \pm 0.011 \mu\text{F}/\text{cm}^2$ and $0.483 \pm 0.029 \mu\text{F}/\text{cm}^2$, respectively; electrical conductivity of the cytoplasm and the vacuole interior were $0.515 \pm 0.028 \text{ S}/\text{m}$ and $3.22 \pm 0.48 \text{ S}/\text{m}$; finally, the permittivity of the cytoplasm was 50.6 ± 2.1 .

Keywords: Electric permittivity; Electric conductivity; Yeast cell

1. Introduction

The studying of dielectric properties of tissues and cell suspensions in the radiofrequency range is important, not only for its implications in medicine, biology and biotechnology [1–7], but also for the fundamental scientific knowledge. Since the pioneering work of Fricke [8], who measured for the first time the capacitance of erythrocyte membranes, the dielectric approach of biological systems has been imposed as a powerful tool for obtaining structural and dynamic information about the cells.

The theories used to model the dielectric behaviour of cell suspensions are essentially based on the dielectric *mixture theory* of Maxwell [9] and Wagner [10], and on the *single(multi)-shell particle model* [11–13]. The single-shell model has been proven to be a good approximation for describing the dielectric behaviour of suspensions of erythrocyte. By using it, reliable values of erythrocyte internal conductivity and permittivity were obtained [14]. Also, the reported values of the membrane capacitance per unit surface [4,14] were in good agreement with those of the solvent-free bilayer lipid membranes (BLM) [15,16].

In spite of this good agreement between theory and experiments on erythrocytes, there is much evidence that the single-shell model no longer applies to the data obtained on suspensions of biological particles comprising intra-membraneous structures. This idea has been supported by the data obtained from dielectric spectroscopic measurements on lymphocytes [4], mitochondria [17] and plant protoplasts [18]. Dielectrophoretic and electrorotation measurements have also shown deviations from spectrum simulated by using the single-shell model (see, for example Ref. [19] and the references therein).

In this paper we report results on yeast cell suspensions. It is well known that yeast cell suspensions show well-defined dielectric dispersion in the 0.1–100 MHz frequency range. Beside the plasma membrane, a cell of yeast possesses also a cell wall and, for a while, it was questionable whether the cell wall does give dielectric dispersion. Asami et al. [20] clearly demonstrated that, in normal physiological conditions, the cell wall makes no contribution to the total dielectric response. Thus, they concluded that the single-shell model can be accepted as far as the electrical parameters of the external medium have the same order of magnitude as the cell wall ones. However, later attempts to interpret the data on yeast revealed the following important problems: (a) a single Cole-Cole function does not fit the high frequency region of the dielectric spectra (this paper);

^{*} Corresponding author. Fax: +40 1 3121147.

¹ Present address: University of Bucharest, Physics Faculty, Department of Electricity and Biophysics, Bucharest-Magurele, Romania.

(b) the Cole-Cole α (0.1–0.3) is too big to be explained in terms of a distribution of cell parameters [21]; (c) the membrane capacitance of some $1.1 \mu\text{F}/\text{cm}^2$, obtained from dielectric spectroscopy [20,22] and also from electro-rotation and dielectrophoresis experiments [23,24], is significantly higher than that of BLM [15,16]; (d) the conductivity of the cell interior (0.2–0.3 S/m [20,22]) is unusually small for biological cells, which are known to have a high protoplasmic ionic content.

Even though these problems were often addressed by the literature, there is still no acceptable explanation for all of them. In our opinion, all the above discrepancies have their origin in the mis-estimation of the dielectric response of the vacuole. This paper aims to demonstrate that the two-shell model provides the best description of the dielectric behaviour of yeast cell suspensions, and offers more reliable phase parameters values than does the single-shell model. The two-shell model used here refers to the cell membrane and the vacuolar membrane, and not to the cell wall, whose dielectric response was experimentally avoided [20].

2. Theoretical statements

2.1. Dielectric behaviour of suspensions of polarizable particles

The dielectric behaviour of suspensions of *homogeneous* particles, when applied an electric field, arises from a build-up of charge at the particle surface (i.e., interfacial polarization). This charge needs time to accumulate and, therefore, its magnitude depends on the rate at which the field changes the sign (i.e., the field frequency). Thus, a suspension of such polarizable particles behaves as an assembly of induced dipoles, its electrical polarization (or, equivalently, its dielectric constant), depending inversely on the frequency of applied field. Mathematically, the dispersion properties (namely, the frequency dependence of the dielectric constant) of a suspension of homogeneous particles can be expressed in terms of the Maxwell-Wagner [9,10] mixture equation:

$$\epsilon_s^* = \epsilon_e^* \frac{(1 + 2\phi)\epsilon_p^* + 2(1 - \phi)\epsilon_e^*}{(1 - \phi)\epsilon_p^* + (2 + \phi)\epsilon_e^*}. \quad (1)$$

In this equation, ϵ^* is the complex dielectric constant, and is defined as $\epsilon^* = \epsilon - j \cdot \sigma/\omega$, where ϵ is the true dielectric constant, σ is the conductivity, ω is the angular frequency of applied field and $j = (-1)^{1/2}$. The indexes s , p and e refer to the suspension, particle and external medium, respectively, and ϕ is the volume fraction of suspended particles.

Eq. (1) correctly predicts the dielectric behaviour of a suspension as long as the field experienced by a particle is not perturbed by the neighbouring particles. This restricts

its applicability to dilute suspensions only. The application of the more rigorous Hanai mixture equation [25] to suspensions of cells requires, however, a more complicated and, thus, discommoding fitting procedure [26]. Besides, Davey et al. [27] demonstrated that Eq. (1) can be safely used up to volume fractions of 0.4, that are well beyond the values used in the present paper ($\phi = 0.2$ –0.25).

It is straightforward to demonstrate [10,28] that Eq. (1) can be put in the form of a Debye dispersion function [29], defined as

$$\epsilon^* = \epsilon_h + \frac{\delta\epsilon}{1 + j\omega\tau} + j\frac{\sigma_l}{\omega} \quad (2)$$

where the indexes h and l stand for high and low frequency, respectively.

2.2. The single-shell particle model

The biological cell is a *heterogeneous* particle, and further assumptions have to be made to derive its equivalent complex dielectric constant. The traditional way of modeling the biological cell is to use the *single-shell* model. Accordingly, the cell is assumed as being conducting homogeneous particle (of complex permittivity ϵ_i^*) covered by a poorly conducting shell (of ϵ_{pm}^*). All the symbols used hereafter are as in Fig. 1, unless specified. Considering the single-shell model, Pauly and Schwan [11] carried out calculus for the complex dielectric constant, ϵ_p^* , of a single-shelled spherical cell, and obtained the following equation:

$$\epsilon_p^* = \epsilon_{pm}^* \frac{(1 + 2v_{pm})\epsilon_i^* + 2(1 - v_{pm})\epsilon_{pm}^*}{(1 - v_{pm})\epsilon_i^* + (2 + v_{pm})\epsilon_{pm}^*} \quad (3)$$

where $v_{pm} = (1 - d_{pm}/R)^3$.

Pauly and Schwan demonstrated that the complex dispersion function of a suspension of single-shelled cells (combination of Eqs. (1) NO TRANSLATION 3)) can be exactly separated into two terms of a Debye-type (Eq. (2)). The interfacial polarization mechanism, discussed above, is responsible for the first sub-dispersion. The second sub-dispersion, which has only a small contribution to the total dielectric response, is accounted for by the so-called [30] ‘Maxwell-Wagner effect’.

2.3. The multi-shell model

Irimajiri et al. [12] generalized the results of Pauly and Schwan to suspensions of spherical particles comprising n concentric shells and showed that the complex dispersion function may be separated into $2n$ Debye terms. The number of sub-dispersions corresponds to the number of interfaces lying between the successive shell phases. Owing to the high complexity of the equations implied, serious difficulties are thought to occur when trying to inter-

pret the dielectric behaviour of multi-shelled particle suspensions. Fortunately, the work on biological systems does not generally require taking into account more than two particle shells. In the case of suspensions of nucleated cells, for example, the two bilayers [31] of the nuclear envelope can be well characterized [4] by a unique set of electrical parameters (i.e., single capacitance and conductance). This means that the experimenter will observe a single dielectric dispersion due to the surface polarization of the nuclear membrane.

According to Irimajiri et al. [12], the complex permittivity of a spherical cell comprising shelled concentric organelle (see Fig. 1b) is given by Eq. (3), with the complex permittivity of the cell interior, ϵ_i^* , expressed as

$$\epsilon_i^* = \epsilon_c^* \frac{(1 + 2v_o)\epsilon_o^* + 2(1 - v_o)\epsilon_c^*}{(1 - v_o)\epsilon_o^* + (2 + v_o)\epsilon_c^*} \quad (4)$$

where v_o is the volume occupied by organelle inside the cell, and is the same with the quantity $\{R_o/(R - d_{pm})\}^3$. The intermediate function ϵ_o^* is expressed by

$$\epsilon_o^* = \epsilon_{om}^* \frac{(1 + 2v_{om})\epsilon_{io}^* + 2(1 - v_{om})\epsilon_{om}^*}{(1 - v_{om})\epsilon_{io}^* + (2 + v_{om})\epsilon_{om}^*} \quad (5)$$

where $v_{om} = (1 - d_{om}/R_o)^3$.

3. Materials and methods

3.1. Preparation and characterization of samples

Yeast cells (Baker's yeast, obtained in house) were grown in liquid cultures, at 27°C, in a medium containing

70 g/l 'Peptone Yeast Extract Agar' (Fluka). Prior to their use, the medium was centrifuged at $1000 \times g$ for 2 min to remove the agar particles. The cells were harvested in the stationary phase after two days and washed twice with distilled water, then suspended in KCl solutions (five concentrations, ranging from 20 to 50 mM). The samples were incubated for 2 h at room temperature and re-suspended in solutions with the corresponding KCl concentrations.

The dimensions of cells and vacuoles were determined over about 100 cells for each sample by measuring them under a phase contrast microscope (magnification: 1050). The cells were spheroidal, with the short and long semi-axis ranging from 2.6 to 3.9 μm and 2.2 to 3.2 μm , respectively. The mean cell radius ($R = 2.95 \pm 0.05 \mu\text{m}$) was calculated from the mean volume of cells by assuming a sphere with the same volume as that of the spheroid. The mean cell radius without the cell wall was calculated using a cell wall thickness of 0.25 μm [32]. Under the phase contrast microscope the cells showed almost spherical sizable vacuole. The mean vacuolar radius was calculated from the mean volume of the vacuoles. Their values were found to change with the concentration of KCl in the external medium (see Table 2 in Section 4).

3.2. Dielectric measurements

Measurements of permittivity and conductivity, over 0.1–100 MHz (50 frequency points), were carried out with a Hewlett Packard impedance-analyzer, model 4194 A. The measuring cell is an open-ended coaxial line, described previously [33]. Cell constant ($k = 0.00235 \text{ m}$) was

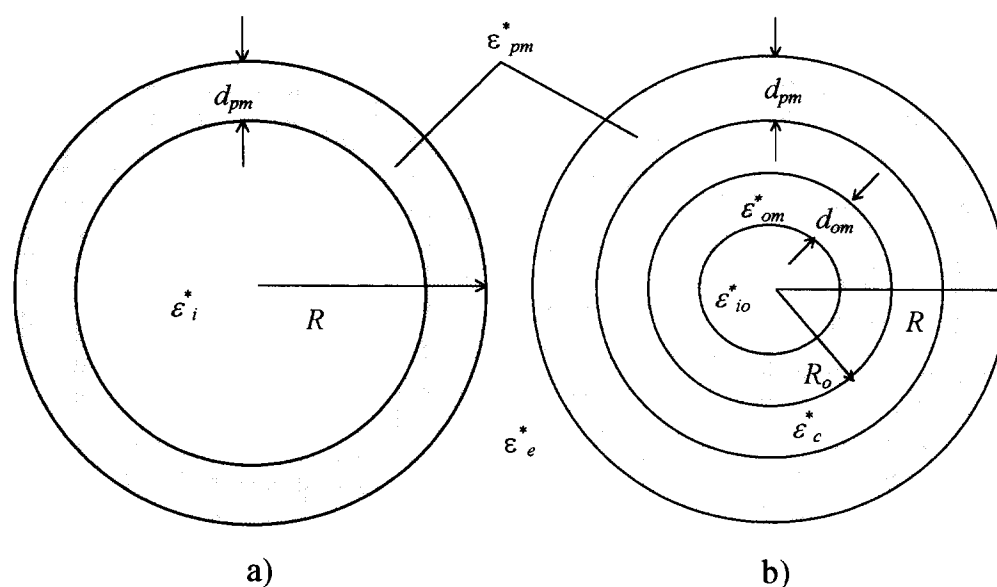


Fig. 1. Single-shell (a) and two-shell models of a cell. ϵ^* is the complex dielectric constant and is defined by $\epsilon^* = \epsilon - j\sigma/\omega$, where ϵ is the permittivity, σ is electrical conductivity, ω is the angular frequency of applied field and $j = (-1)^{1/2}$. The subscripts 'pm' and 'om' refer to the plasma membrane and the organelle membrane, respectively, while 'e', 'c' and 'io' stand for the external medium, the cytoplasm and the interior of organelle. The other symbols have their apparent meanings.

determined by calibration with NaCl solutions of known conductivity and permittivity [34]. Accuracy of permittivity and conductivity data was within a few percent. The medium conductivity was measured, immediately after dielectric measurements, by removing the cells from suspensions. All measurements were made at room temperature ($21 \pm 1^\circ\text{C}$).

3.3. Curve-fitting procedure

Theoretical curves were fitted to the data by using a computer. The rough fitting was achieved by visually comparing the curves to the data. The best-fit parameters were searched manually, in order to minimize the functional

$$\text{Dev}(\epsilon, \sigma) = \left(\sum_i (\epsilon_{ti} - \epsilon_{di})^2 / \sum_i \epsilon_{di}^2 + \sum_i (\sigma_{ti} - \sigma_{di})^2 / \sum_i \sigma_{di}^2 \right)^{1/2} \quad (6)$$

where ϵ and σ are suspension permittivity and conductivity, and indexes t and d stand for theoretical and experimentally determined values, respectively. Volume fraction, ϕ , was calculated [11] from the equation:

$$\phi = 2 \frac{1 - \sigma_i/\sigma_e}{2 + \sigma_i/\sigma_e} \quad (7)$$

where the suspension limiting conductivity at low frequency was obtained by fitting the data with a Cole-Cole function (see below). Morphological cell parameters (R , R_o , d_{pm} , d_{om} , see Fig. 1) and volume fraction were taken as constants when fitted the two-shell model to the data.

4. Results

4.1. Choosing of the appropriate electrical cell model

Fig. 2 shows typical permittivity and conductivity data obtained in measurements on yeast cell suspensions. The conductivity of external medium was chosen such as to avoid the interference between the dielectric signal of cell wall and the β dielectric dispersion under study [20,22]. The steep rise of permittivity as frequency decreased was due to the electrode polarization phenomena, and was corrected as explained elsewhere [33].

As is customarily made in studies on suspensions of yeast, we firstly tried to simulate the data by means of a single Cole-Cole [35] dispersion function:

$$\epsilon^* = \epsilon_h + \frac{\delta\epsilon}{1 + (j\omega\tau)^{1-\alpha}} + j \frac{\sigma_l}{\omega} \quad (8)$$

The Cole-Cole α ($0 < \alpha < 1$) is a measure of the devia-

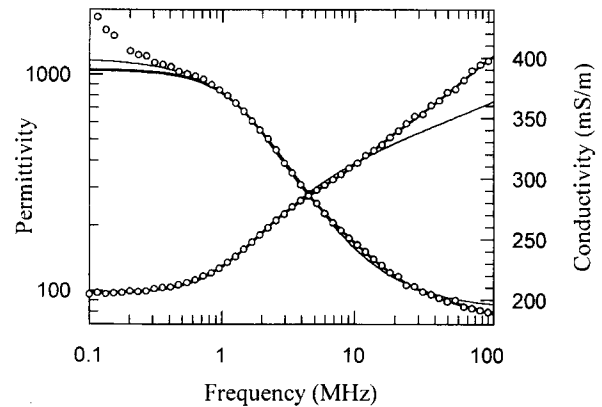


Fig. 2. Frequency dependence of permittivity and conductivity of yeast cell suspension. Suspending medium was 25 mM KCl solution ($\sigma_e = 0.301$ S/m), volume fraction, ϕ , was 0.238, cell radius, $2.93 \mu\text{m}$ and measuring temperature, $21 \pm 1^\circ\text{C}$. The thin lines represent theoretical curves predicted by the Cole-Cole function, while the thick ones were simulated with a sum of three Debye-type function (see text). The best-fit phenomenological parameters are given in Table 1.

tion of data from an ideal Debye spectrum given by Eq. (2). It can be readily seen in Fig. 2 and Table 1 that the Cole-Cole function failed to describe our data in the high frequency range. Furthermore, the breadth of the dielectric dispersion in the megahertz region, as reflected by the Cole-Cole α ($= 0.120$), seems to be too large. The same was remarked by Markx et al. [21] in measurements on dilute yeast cell suspensions. These authors demonstrated that such a breadth of the β dispersion cannot be solely explained in terms of the distribution of phase parameters of cells. Consequently, our work hypothesis was that the large value of α appears from the overlapping of two distinct dispersions. Moreover, to simulate the data in the high frequency range, one more sub-dispersion had to be considered.

Taking into account all the above statements, we next tried to simulate the data with a sum of three Debye functions. As can be readily seen in Fig. 2, the fitting was excellent over the whole frequency range.

One can conclude, at this stage, that the β dispersion of yeast cells is a composite of at least three distinct sub-dispersions, and this seems to be the best explanation of the large value found for the Cole-Cole α . It is to be noted that such a behaviour is characteristic to all the biological particles comprising intra-membraneous structures [4,17,18].

Table 1
Dielectric parameters of theoretical curves in Fig. 2

σ_l (S/m)	$\delta\epsilon_1$	f_{c1} (MHz)	$\delta\epsilon_2$	f_{c2} (MHz)	$\delta\epsilon_3$	f_{c3} (MHz)	ϵ_h
0.205	1110	1.59	—	—	—	—	82.9
0.206	888	1.69	87	12.50	19	70.32	68.1

First row: single Cole-Cole function. Second row: three Debye-type functions.

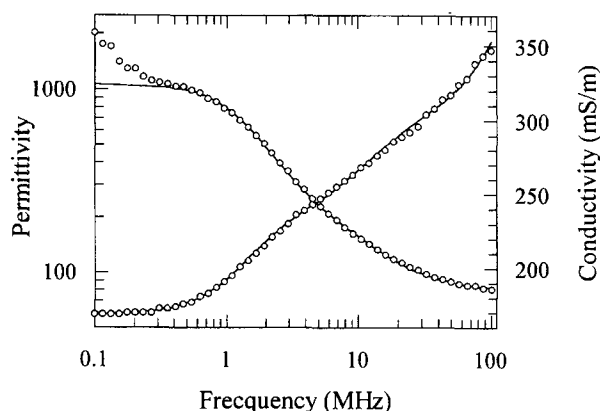


Fig. 3. Experimental data and theoretical simulations based on the two-shell model. Yeast cells were suspended in 20 mM KCl solution ($\sigma_e = 0.250$ S/m) at a volume fraction of 0.223. Measuring temperature was $21 \pm 1^\circ\text{C}$. Electrical phase parameters were listed in Table 2.

According to the model of Irimajiri et al. [12,13], suspensions of yeast cells in the stationary phase should exhibit *four* sub-dispersions owing to the presence of vacuole inside the cell. The *three* sub-dispersions observed in our analysis may be ascribed to the plasma membrane, the vacuolar membrane and the cytoplasm, respectively. Unfortunately, we were not able to detect the fourth sub-dispersion corresponding to the vacuolar interior. This was probably due to the fact that its characteristic frequency has a value (dictated roughly by the ratio $\sigma_{i_o}/\epsilon_{i_o}$) much higher than the highest frequency used in the present work (100 MHz). This seems indeed to be the case, since the conductivity of vacuolar content obtained from our analysis below has a very large value.

4.2. Analysis based on the two-shell model

Following the curve-fitting procedure described in Section 3 and considering the two-shell model, it is possible to determine the average phase parameters if the morphological cell parameters are available. Fig. 3 shows the best fit curves obtained with the two-shell model. As can be seen, the model gave an excellent fitting, for both permittivity and conductivity data.

For further examination of the two-shell model, the KCl concentration of the external medium was varied between 20 mM and 50 mM. Numerical results obtained were summarized in Table 2. As can be seen, the salt content of the external medium significantly influenced the mean radius of vacuole (R_o) and the conductivity of cytoplasm (σ_c) and vacuole interior (σ_{i_o}). It can be seen that the conductivity of both cytoplasm and vacuole content has remarkably high values, even for low medium conductivity.

5. Discussion

As was demonstrated in Section 4 of this paper, the large value of α Cole-Cole appears from the overlapping of two relatively close sub-dispersions. While the first sub-dispersion was undoubtedly related to the interfacial polarization of the plasma membrane, the second one was ascribed by us to the polarization of the vacuole membrane. It must be mentioned, as support for the last consideration, that the vacuole is the organelle [36] that occupies the largest volume of the yeast cell interior (average volume fraction = 0.2). Markx et al. [21] recorded changes in the α Cole-Cole during the batch culture of yeast. The largest value was of about 0.3 for the culture in the exponential phase, while the smallest one was close to 0.2 for culture in the stationary phase. On the other hand, yeast cytological studies have shown [36] that for cultures in the exponential phase the vacuolar content disseminates into many small vacuoles. In such a case, the interior of yeast cells can be depicted as a 'suspension' of organelles having an increased relaxation frequency, as compared to the case of a single larger vacuole in the stationary phase (owing to the inverse proportionality between relaxation frequency and radius [11]). In the light of our interpretation above, this would result in an increase of α Cole-Cole in the exponential phase relative to the stationary phase.

The capacitance of plasma membrane ($C_m = 0.703 \pm 0.011 \mu\text{F}/\text{cm}^2$) obtained from our analysis compared well to that of solvent-free BLM ($0.73 \mu\text{F}/\text{cm}^2$ [15]; $0.76 \mu\text{F}/\text{cm}^2$ [16]) and also to that of erythrocyte membrane

Table 2
Electrical phase parameters for yeast cells dispersed in solutions with various concentrations of KCl

KCl (mM)	σ_e (S/m)	R_o (μm)	σ_c (S/m)	ϵ_c	C_{pm} ($\mu\text{F}/\text{cm}^2$)	σ_{i_o} (S/m)	C_{om} ($\mu\text{F}/\text{cm}^2$)	Dev/100
20	0.250	1.90	0.464	53	0.718	2.45	0.440	2.00
25	0.301	1.83	0.520	47	0.714	2.88	0.486	1.96
30	0.362	1.81	0.546	50	0.699	3.68	0.516	2.03
40	0.475	1.72	0.510	52	0.693	3.47	0.460	2.01
50	0.587	1.70	0.534	51	0.692	3.60	0.511	1.91

Morphological parameters were: $R = 2.95 \mu\text{m}$, $d_{pm} = d_{om} = 2.5$ nm. The two membrane capacitances were calculated from the formula: $C_m = \epsilon_i \epsilon_m / d$, where $\epsilon_i = 8.854 \cdot 10^{-12}$ F/m. Assumed dielectric constant of external medium: $\epsilon_e = 80$.

($0.72 \mu\text{F}/\text{cm}^2$ [4]; $0.74 \mu\text{F}/\text{cm}^2$ [14]). By analogy to the dielectric properties of BLM [37], one can consider that the capacitance of the membrane polar layers are much larger than the capacitance of the hydrocarbon layer. Therefore, the membrane dielectric response is probably dominated by its hydrophobic layer. If a value of 25 \AA is assumed for the thickness of the nonpolar core [32], the measured capacitance corresponds to a dielectric constant of 1.99 ± 0.03 . This value agrees well to that of some 2.1 permittivity units obtained in studies on BLM [16,37].

As was pointed out in Section 4, the electrical conductivity of cytoplasm (in between 0.464 and 0.546 S/m) has larger values than reported, for example, by Asami et al. (0.22 – 0.35 S/m [20]). This is, in fact, an expected finding, since the single-shell model used so far does not take into account the insulating properties of the vacuolar membrane inside the cell.

The mean value obtained for the capacitance of the vacuolar envelope was surprisingly small ($C_{om} = 0.483 \pm 0.029 \mu\text{F}/\text{cm}^2$). It is probably an approximate value, since in the model used, the dielectric response of some other cytoplasmic organelles (such as nucleus) vanishes.

The conductivity of vacuole interior was $3.22 \pm 0.48 \text{ S/m}$, a value that is much higher than that of the cytoplasm. This could be due to the difference between the water contents of the cytoplasm and vacuole interior.

The cytoplasm permittivity obtained in this work ($\epsilon_c = 50.6 \pm 2.1$) was in good agreement to the ones obtained by other authors [20,22], while the permittivity of the nuclear plasma was inaccessible for our measurements, which are limited to 100 MHz in upper frequency.

To conclude, one can say that the two-shell model gave reliable information about yeast cells. This paper proved that the two-shell model is a better approximation for yeast cells, as compared to the single-shell model, even if the two major sub-dispersions found (corresponding to the cell membrane and the vacuolar membrane) could not be visually distinguished from each other.

References

- [1] Swarup, A., Stuchly, S.S. and Surowiec, A. (1991) *Bioelectromagnetics* 12, 1–18.
- [2] Ballario, C., Bonincontro, A. and Cametti, C. (1984) *Z. Naturforsch.* 39c, 1163–1169.
- [3] Asami, K., Hanai, T. and Koizumi, N. (1980) *Biophys. J.* 31, 215–228.
- [4] Asami, K., Takahashi, Y. and Takashima, S. (1989) *Biochim. Biophys. Acta* 1010, 49–55.
- [5] Davey, C.L., Kell, D.B., Kemp, R.B. and Meredith, R.W.J. (1988) *Bioelectrochem. Bioenerg.* 20, 83–98.
- [6] Davey, C.L., Davey, H.M., Kell, D.B. and Tod, R.W. (1993) *Anal. Chim. Acta* 279, 155–161.
- [7] Davey, C.L., Markx, G.H. and Kell, D.B. (1993) *Pure and Appl. Chem.* 65, 1921–1926.
- [8] Fricke, H. (1925) *Phys. Rev.* 26, 682–687.
- [9] Maxwell, J.C. (1891), *A Treatise on Electricity and Magnetism*, Vol.1, Clarendon Press, Oxford.
- [10] Wagner, K.W., (1914) *Arch. Elektrotech.* 2, 371–387.
- [11] Pauly, H. and Schwan, H.P. (1959) *Z. Naturforsch.* 14b, 125–131.
- [12] Irimajiri, A., Hanai, T. and Inouye, A. (1979) *J. Theor. Biol.* 78, 251–269.
- [13] Irimajiri, A., Doida, Y., Hanai, T. and Inouye, A. (1978) *J. Membr. Biol.* 38, 209–232.
- [14] Kaneko, H., Asami, K. and Hanai, T. (1991) *Colloid Polym. Sci.* 269, 1039–1044.
- [15] Benz, R. and Janko, K. (1976) *Biochim. Biophys. Acta* 455, 721–738.
- [16] Fettiplace, R. (1978) *Biochim. Biophys. Acta* 513, 1–10.
- [17] Asami, K. and Irimajiri, A. (1984) *Biochim. Biophys. Acta* 778, 570–578.
- [18] Asami, K. and Yamaguchi, T. (1992) *Biophys. J.* 63, 1493–1499.
- [19] Gimsa, J., Marszalek, P., Loewe, U. and Tsong, T.Y. (1991) *Biophys. J.* 60, 749–760.
- [20] Asami, K., Hanai, T. and Koizumi, N. (1976) *J. Membrane Biol.* 28, 169–180.
- [21] Markx, G.H., Davey, C.L. and Kell, D.B. (1991) *Bioelectrochem. Bioenerg.* 25, 195–211.
- [22] Asami, K. (1977) *Bull. Inst. Chem. Res. Kyoto Univ.* 55, 394–414.
- [23] Huang, Y., Hölzel, R., Pethig, R. and Wang, X.-B. (1992) *Phys. Med. Biol.* 37, 1499–1517.
- [24] Hölzel, R. and Lamprecht, I. (1992) *Biochim. Biophys. Acta* 1104, 195–200.
- [25] Hanai, T. (1960) *Kolloid Z.* 171, 23–31.
- [26] Hanai, T., Asami, K. and Koizumi, N. (1979) *Bull. Inst. Chem. Res. Kyoto Univ.* 57, 297–305.
- [27] Davey, C.L., Davey, H.M. and Kell, D.B. (1992) *Bioelectrochem. Bioenerg.* 28, 319–340.
- [28] Wang, X.-B., Huang, Y., Hölzel, R., Burt, J.P.H. and Pethig, R. (1993) *J. Phys. D: Appl. Phys.* 26, 312–322.
- [29] Debye, P. (1945) *Pollar Mollecules*, Dover Publications, London.
- [30] Schwan, H.P. (1988) *Ferroelectrics*, 86, 205–223.
- [31] Worman, H.J., Evans, C.D. and Blobel, G. (1990) *J. Cell Biol.* 111, 1535–1542.
- [32] Vitols, E., North, R.J., Linnane, A. (1961) *J. Biophys. Biochem. Cytol.* 9, 689–699.
- [33] Raicu, V. (1995) *Meas. Sci. Technol.* 6, 410–414.
- [34] Stogryn, A. (1971) *IEEE Trans. Microwave Theory Tech.* 19, 733–736.
- [35] Cole, K.S. and Cole, R.H. (1941) *J. Chem. Phys.* 9, 341–351.
- [36] Anghel, I., Voica, C., Toma, N. and Cojocaru, I. (1993), *Biology and Technology of Yeasts (in Romanian)*, Vol.1, Ed. Tehnica, Bucharest.
- [37] Ashcroft, R.G., Coster, H.G.L. and Smith, J.R. (1981) *Biochim. Biophys. Acta* 643, 191–204.